WIND TUNNEL TESTS OF THREE CANDIDATE MK 82 SNAKEYE BOMB REPLACEMENT CONFIGURATIONS

William J. Miklos, et al

Aerospace Research Laboratories
Wright-Patterson Air Force Base, Ohio

June 1975

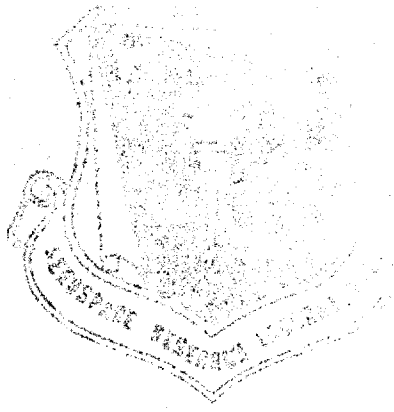

WIND TUNNEL TESTS OF THREE CANDIDATE MK 82 SNAKEYE BOMB REPLACEMENT CONFIGURATIONS

FLUID MECHANICS RESEARCH LABORATORY/ARL
TECHNOLOGY INCORPORATED
P.O. BOX 3036, OVERLOOK BRANCH
DAYTON, OHIO 45431

JUNE 1975

INTERNAL REPORT SEPTEMBER 1974 — FEBRUARY 1975

UNCLASSIFIED

SECURITY CLASSIFICATION OF THIS PAGE (When Data Entered)

REPORT DOCUMENTATION PAGE		READ INSTRUCTIONS BEFORE COMPLETING FORM
1 REPORT NUMBER ARL 75-0174	2 GOVT ACCESSION NO.	3 RECIPIENT'S CATALOG NUMBER
4 TITLE (and Subtitle) Wind Tunnel Tests of Three Candidate MK 82 Snakeye Bomb Replacement Configurations		5 TYPE OF REPORT & PERIOD COVERED Technical - Interim Sep 74 - Feb 75 6 PERFORMING ORG. REPORT NUMBER
7 AUTHOR(s) William J. Miklos, 2Lt, USAF Charles W. Ingram		8 CONTRACT OR GRANT NUMBER(s)
9 PERFORMING ORGANIZATION NAME AND ADDRESS Fluid Mechanics Research Laboratory Aerospace Research Laboratories (AFSC) Wright-Patterson AFB, Ohio		10 PROGRAM ELEMENT, PROJECT, TASK AREA & WORK UNIT NUMBERS DoD Element 61102F Project 70651125
11 CONTROLLING OFFICE NAME AND ADDRESS Aerospace Research Laboratories (LF) Air Force Systems Command Wright-Patterson AFB, OH 45433		12 REPORT DATE June 1975 13 NUMBER OF PAGES 30
14 MONITORING AGENCY NAME & ADDRESS(if different from Controlling Office)		15 SECURITY CLASS. (of this report) Unclassified 15a DECLASSIFICATION DOWNGRADING SCHEDULE

16 DISTRIBUTION STATEMENT (of this Report)

Approved for public release; distribution unlimited.

17 DISTRIBUTION STATEMENT (of the abstract entered in Block 20, if different from Report)

18 SUPPLEMENTARY NOTES

19 KEY WORDS (Continue on reverse side if necessary and identify by block number)

static stability
damping stability
bombs
aerodynamic coefficients
wind tunnel testing
bomb aerodynamics

20 ABSTRACT (Continue on reverse side if necessary and identify by block number)

Static and pitch damping moment stability coefficients are presented for three candidate MK 82 Snakeye Bomb replacement configurations as functions of Mach number. The normal force coefficient slope, C_{N_α}, and the center of pressure are also determined for each design. All coefficients are measured at a Mach number of .13 in the subsonic tunnel of AFATL and at Mach numbers of .5 and .8 in the transonic pilot tunnel of the NSRDC. The restoring moment stability coefficient, normal force coefficient slope, and center of pressure of the

DD FORM 1 JAN 73 1473 EDITION OF 1 NOV 65 IS OBSOLETE

SECURITY CLASSIFICATION OF THIS PAGE (When Data Entered)

Fixed Fin design are also measured at transonic Mach numbers at AEDC. The Inflatable Stabilizer Retarder configurations are found to have more static and pitch damping stability than the Fixed Fin design.

PREFACE

This report was prepared by 2Lt. William J. Miklos of the Fluid Mechanics Research Laboratory, Aerospace Research Laboratories of Air Force Systems Command,and Dr. Charles W. Ingram, visiting scientist at Aerospace Research Laboratories employed through Technology Incorporated. The work described herein was requested by Air Force Armament Laboratory and was accomplished between September 1974 and February 1975. Mr. Paul D. Shirey of Armament Laboratory served as program manager.

TABLE OF CONTENTS

LIST OF FIGURES

SECTION I

INTRODUCTION

Air Force Armament Laboratory (AFATL) has requested that the Aerospace Research Laboratories (ARL) assist in the aerodynamic evaluation of three replacement designs for the MK 82 Snakeye Bomb. The purpose of this report is to document a series of subsonic dynamic wind tunnel tests carried out at AFATL, transonic dynamic wind tunnel tests conducted at the Naval Ship Research and Development Center (NSRDC), and transonic static tests accomplished at Arnold Engineering Development Center (AEDC) to determine the aerodynamic characteristics of the candidate configurations.

The Snakeye Bomb depicted in Figure 1 is an aircraft store which may operate in either a high or low drag flight mode. However, the transonic static instability of the low drag mode [1,2] and the mechanical unreliability of the high drag mode have necessitated the design and evaluation of a new weapon to fulfull this dual mode mission requirement. Although the three candidate replacements have this capability, the mechanical fin decelerator system of the Snakeye has been replaced by a ram air inflatable retarder.[3,4] This retarder is stored in the stabilizer assembly of the bomb and is deployed when the weapon has separated from the aircraft.

The three low drag candidate configurations which were tested are depicted in Figure 2. While they consist of the same six caliber forebody, they differ in the design of their tail assemblies. The two basic configurations shown in this figure result from the aircraft carriage requirement that the tip-to-tip fin span be no greater than 1.4 times the maximum body diameter. The first of these designs employs a fixed cruciform finned tail section similar to that of the Low Drag Bomb with the exception that it has no boattailing and an increased fin chord. The other basic shape, the ISR, utilizes an inflatable stabilizer. The tail assembly of this design is folded for aircraft carriage and, upon release, is deployed to the low drag configuration shown in the figure. The third shape simply results from the addition of an extender to the second basic design. All three configurations will employ the same ram air inflatable decelerator for the high drag flight mode.

Single degree of freedom free-oscillation wind tunnel tests were conducted at AFATL and NSRDC to obtain the static moment stability coefficient, C_{M_α}, and the damping moment stability coefficient, $C_{M_q} + C_{M_{\dot{\alpha}}}$. These coefficients were determined as functions of center of gravity position for all candidate shapes at the following Mach numbers: 0.13, 0.5 and 0.8. The normal force coefficient slope, C_{Z_α}, and the center of pressure location of each configuration were determined from the C_{M_α} versus center of gravity position data. Static tests of the Fixed Fin design were also carried out at AEDC to confirm the results of the AFATL and NSRDC tests and to better define the aerodynamic characteristics of this configuration at higher Mach numbers. Force and moment measurements at the flight center of gravity were obtained at Mach numbers of 0.3, 0.5, 0.8, 0.9, 0.95, and 1.0.

SECTION II

THEORY

During the AFATL and NSRDC dynamic tests, the model was supported by a vertical strut which restricts its angular oscillation to the yaw plane. As a result, the motion was not affected by any moments created if the center of gravity did not lie below the strut centerline. The dynamics is therefore comparable to a model freely pitching in a wind tunnel while supported at its center of gravity. If the mount contributes negligible friction forces, the angular motion is governed by the three forces and their moments depicted in Figure 3. These forces are referred to as the static force, damping force, and aerodynamic lag force and are denoted by (5)

$$\text{(static)} \quad Z_\alpha\alpha = C_{Z_\alpha}\,\alpha\,QS \qquad (1)$$

$$\text{(damping)} \quad Z_q q = C_{Z_q}\,\frac{qd}{2V}\,QS \qquad (2)$$

$$\text{(lag)} \quad Z_{\dot\alpha}\dot\alpha = C_{Z_{\dot\alpha}}\,\frac{\dot\alpha d}{2V}\,QS \qquad (3)$$

The moments of these forces about the center of gravity (or pivot point in this case) are described by the following equations:

$$\text{(static)} \quad M_\alpha\alpha = C_{M_\alpha}\alpha\,QSd \qquad (4)$$

$$\text{(damping)} \quad M_q q = C_{M_q}\,\frac{qd}{2V}\,QSd \qquad (5)$$

$$\text{(lag)} \quad M_{\dot\alpha}\dot\alpha = C_{M_{\dot\alpha}}\,\frac{\dot\alpha d}{2V}\,QSd \qquad (6)$$

Aeroballisticians have resolved that the damping moment and the lag moment cannot be measured separately, and therefore Eqs(5) and (6) are always written in a coupled form. The equations which are essential to a single degree of freedom stability analysis of a body with no aerodynamic asymmetries are therefore

$$M_\alpha\alpha = C_{M_\alpha}\,\alpha\,QSd \qquad (7)$$

$$(M_q+M_{\dot\alpha})\,\dot\alpha = (C_{M_q}+C_{M_{\dot\alpha}})\,\frac{\dot\alpha d}{2V}\,QSd \qquad (8)$$

It is now possible to formulate the differential equation whose solution will describe the oscillation of the body. From Newton's Second Law

$$I_y\ddot\alpha = \sum M \qquad (9)$$

Substituting the expressions for the static moment and the damping moment, one obtains the desired result,

$$I_y \ddot{\alpha} = M_\alpha \alpha + (M_q + M_{\dot{\alpha}})\ \dot{\alpha} \tag{10}$$

or in another form

$$\ddot{\alpha} - \left(\frac{M_q + M_{\dot{\alpha}}}{I_y}\right)\ \dot{\alpha} - \frac{M_\alpha}{I_y}\ \alpha = 0 \tag{11}$$

The solution to this linear, second order, homogeneous differential equation is a damped cosine function:

$$\alpha\ (t) = \alpha_0\ e^{\lambda t}\ \cos(\omega t + \delta) \tag{12}$$

where

$$\lambda = \frac{M_q + M_{\dot{\alpha}}}{2I_y} \tag{13}$$

and

$$\omega = \sqrt{-\frac{M_\alpha}{I_y}} \tag{14}$$

Using Eqs (7) and (8) the above expressions for the damping rate and frequency become

$$\lambda = (C_{M_q} + C_{M_{\dot{\alpha}}})\ \frac{QSd}{4I_y V} \tag{15}$$

and

$$\omega = \sqrt{-\frac{C_{M_\alpha} QSd}{I_y}} \tag{16}$$

A body is said to possess static stability when

$$C_{M_\alpha} < 0 \tag{17}$$

and is said to possess damping stability when

$$C_{M_q} + C_{M_{\dot{\alpha}}} < 0 \tag{18}$$

SECTION III

EXPERIMENTAL PROCEDURE

In both the AFATL and NSRDC dynamic tests, the free-oscillation technique was used to obtain data required to extract the desired aerodynamic coefficients. Schematics of the two test section support systems are presented in Figures 4 and 5. The models were manually displaced to a high angle of attack orientation, and, after they were released, the subsequent motion of the pointers was photographed by a high speed camera. These photographic data were then analyzed to determine the circular frequency and damping rate of the oscillation.

The AFATL subsonic wind tunnel is an open circuit facility which utilizes a radial blower to force ambient air through the 3 x 5 foot test section. While the maximum attainable velocity is 190 feet per second, all dynamic tests were conducted at approximately 150 feet per second. In order to insure that sufficient data were available to determine the normal force characteristics, the three configurations were tested with the pivot point located at 3.154 diameters, 3.655 diameters (ISR flight center of gravity), and 3.934 diameters (Fixed Fin flight center of gravity)from the nose of the model. The required transverse moments of inertia were calculated from torsional pendulum data obtained at the Measurements Laboratory of the Ballistic Aerodynamics Research System of AFATL.

Stability data at higher Mach numbers were collected in the closed circuit, single return, 5x 7 inch wind tunnel of the NSRDC. As depicted in Figure 5, the top and bottom walls are slotted to allow the flow to expand into a pressure chamber which surrounds the test section. During tunnel operation, the total pressure in the circuit was set at 1100.0 pounds per square foot, and the total temperature reached a maximum of 98°F at M = 0.8. Each configuration was tested with the vertical strut located at axial stations which were 3.655 diameters and 3.934 diameters from the nose. The transverse moments of inertia of the 0.625 inch diameter models were calculated at ARL by the torsional pendulum method.

Further static tests of the Fixed Fin configuration were accomplished at AEDC in the four foot transonic tunnel of the Propulsion Wind Tunnel Facility. Since this closed circuit, variable density tunnel is designed to operate over a Mach number range from 0.1 to 1.3, its test section is equipped with variable pourosity walls to control flow blockage and shock wave interference. The one-fifth scale model which was tested in the AFATL tunnel was also used during these transonic tests after it was modified to be compatible with the existing sting support equipment. Aerodynamic forces and moments were measured by an internally mounted six component strain gauge balance and the electrical output was analyzed by an on-line Ratheon 520 computer. A more complete description of the tunnel and its associated equipment may be found in Reference 6.

SECTION IV

ANALYSIS PROCEDURE

The dynamic test data collected at AFATL and NSRDC were analyzed at ARL using a mathematical technique which will be developed in this section. The method relates the frequency of oscillation, the angular damping rate, and other physical parameters to the desired aerodynamic coefficients. The circular frequency of the motion may be defined in terms of the period of oscillation,

$$\omega = \frac{2\Pi}{T} \tag{19}$$

When ω is computed for each cycle, the values are averaged and the result is used in the calculation of the static coefficient.

A rearrangement of Eq (14) yields

$$M_\alpha = - \omega^2 I \tag{20}$$

where the value of I is the transverse inertia of the model plus the axial inertia of the attached vertical strut. It is also true that

$$M_\alpha = C_{M_\alpha} QSd \tag{21}$$

Equating these expressions yields the desired equation which relates the angular frequency to the static moment stability coefficient,

$$C_{M_\alpha} = - \omega^2 \frac{I}{QSd} \tag{22}$$

After the aerodynamic trim angle and any pointer misalinements have been removed from the angular data, the oscillation extrema may be connected by a curve which is described by the following equation:

$$\alpha_m (t) = \alpha_o e^{\lambda(t-t_o)} \tag{23}$$

Taking the natural log of this expression and rearranging yield

$$\lambda = \frac{\ell n\ \alpha_m (t) - \ell n\ \alpha_o}{t - t_o} \tag{24}$$

Therefore, simply calculating the slope of the line drawn through the $\ell n\ \alpha_m$, t points yields the value of λ. Figure 6 is typical of the plots generated by this method. From Eq (13) it is found that

$$M_q + M_{\dot\alpha} = 2I\lambda \tag{25}$$

Equating the above expression with Eq (8) yields

$$C_{M_q} + C_{M_{\dot{\alpha}}} = \lambda \frac{4IV}{QSd^2} \tag{26}$$

The desired coefficients may be determined from Eqs (22) and (26).

After C_{M_α} has been determined at each center of gravity location, it becomes possible to calculate the value of the normal force coefficient slope and the center of pressure location [7]. In Figure 7 it may be seen that the moment with respect to a pivot at the axial station X_{CG} is defined by the following equation:

$$C_M QSd = C_Z QS\ (X_{CG}-X_{CP}) \tag{27}$$

or

$$C_M = C_Z \frac{X_{CG}-X_{CP}}{d} \tag{28}$$

Accordingly, the moment coefficient C_M^* referred to a pivot center at axial station $X_{CG} + \Delta X$ is

$$C_M^* = C_Z \frac{X_{CG}+\Delta X-X_{CP}}{d} \tag{29}$$

Subtracting Eq (28) from Eq (29) and rearranging yield

$$C_Z = \frac{C_M^*-C_M}{\Delta X/d} \tag{30}$$

Since C_Z and C_M are functions of angle of attack, the above equation may be differentiated with respect to α:

$$C_{Z_\alpha} = \frac{C_{M_\alpha}^*-C_{M_\alpha}}{\Delta X/d} \tag{31}$$

where the moment stability derivatives are obtained from two free oscillation tests with the pivot located at the two axial stations X_{CG} and $X_{CG} + \Delta X$. Therefore, on a C_{M_α} versus X_{CG}/d plot, the slope of a line drawn through the data points yields C_{Z_α}.

The distance between the pivot point and the aerodynamic center of pressure is now obtained by using Eq (28) and differentiating with respect to angle of attack:

$$\frac{X_{CG}-X_{CP}}{d} = \frac{C_{M_\alpha}}{C_{Z_\alpha}} \qquad (32)$$

Since the analysis of the transonic data was accomplished by AEDC personnel, a detailed discussion of their computerized reduction techniques is neither required nor desirable. However, it should be noted that the values of the static moment stability coefficient were obtained by fitting a line through the C_M versus α data points at -2°, 0°, and 2° angles of attack.

SECTION V

RESULTS

Figure 8 presents the restoring moment stability coefficient as a function of Mach number for all three candidate configurations at their nominal flight centers of gravity. In addition, data collected by the Naval Ordnance Laboratory pertaining to the Low Drag Bomb [8] is plotted for comparison. Despite the geometrical similarities between the Fixed Fin and the Low Drag Bomb, the Fixed Fin does exhibit less static stability. This is due, in part, to the forward movement of the center of pressure on that design as a result of the longer fin chord. Concerning the Fixed Fin data, good repeatability has been obtained between the NSRDC dynamic test data and the results of the static tests conducted at AEDC. This figure also shows that the ISR configuration has a more negative restoring moment stability coefficient than the Fixed Fin due to the larger fin span of the former. The addition of the extender to the ISR design moved the fin lift force rearward causing a further increase in the absolute magnitude of the static moment stability coefficient.

In Figure 9 the damping moment stability coefficient is plotted versus Mach number for the candidate configurations and the Low Drag Bomb at their flight centers of gravity. The longer fin span of the ISR design generates damping moments which are more negative than those of the Fixed Fin although this candidate does possess adequate stability. The difference between the damping coefficient of the Fixed Fin and the Low Drag Bomb may be attributable to the larger fin area and wider afterbody of the former. As may be expected, the addition of the extender to the ISR design effects more negative pitch damping moment coefficients.

The normal force coefficient slope, $C_{Z\alpha}$, is presented in Figure 10 as a function of Mach number for the three candidate configurations and the Low Drag Bomb. The slight variation between the Fixed Fin static and dynamic test results may be caused by the different types of data acquisition and analysis techniques employed. The less exact method used to extract the coefficient from the dynamic data is believed to cause a significant portion of the difference exhibited. As shown in the figure, the ISR configurations have more negative normal force coefficient slopes than the Fixed Fin design.

The center of pressure locations of the four bomb configurations as a function of Mach number appear in Figure 11. The effect of the longer fin chord of the Fixed Fin design is again evident as this configuration exhibits the most forward center of pressure. Because of the addition of the extender, the center of pressure of the ISR-E is more rearward than that of the ISR.

SECTION VI

CONCLUSIONS AND RECOMMENDATIONS

Static and dynamic wind tunnel tests of the Fixed Fin, ISR, and ISR-E candidate Snakeye Bomb replacements have shown that the normal force coefficient slope and the static and damping moment stability coefficients of the ISR designs are more negative than those of the Fixed Fin. However, this variation in magnitude of the aerodynamic stability coefficients is not a sufficient criterion for eliminating any design as a potential replacement. Additional Magnus and roll stability tests should be accomplished and the results utilized in analytical stability evaluations before a decision is made.

LOW DRAG MODE

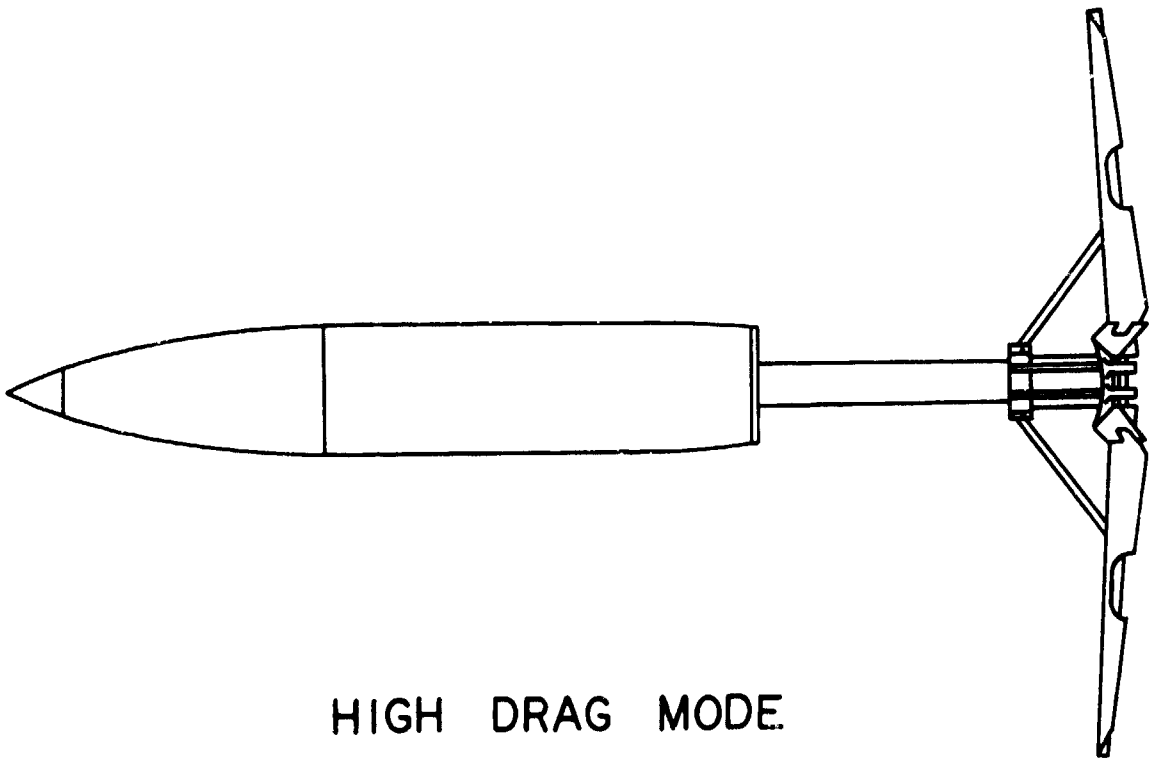

HIGH DRAG MODE

Figure 1. MK 82 Snakeye Bomb

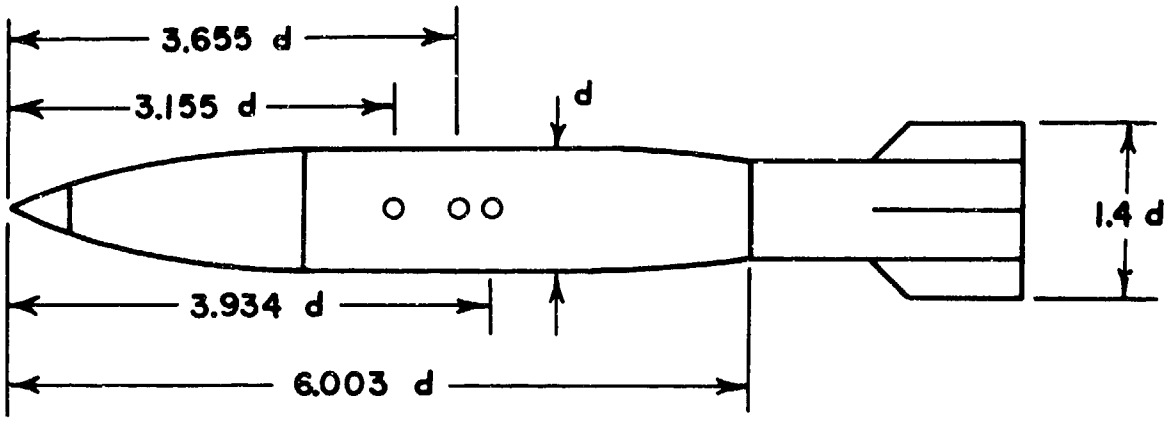

FIXED FIN
(FF)

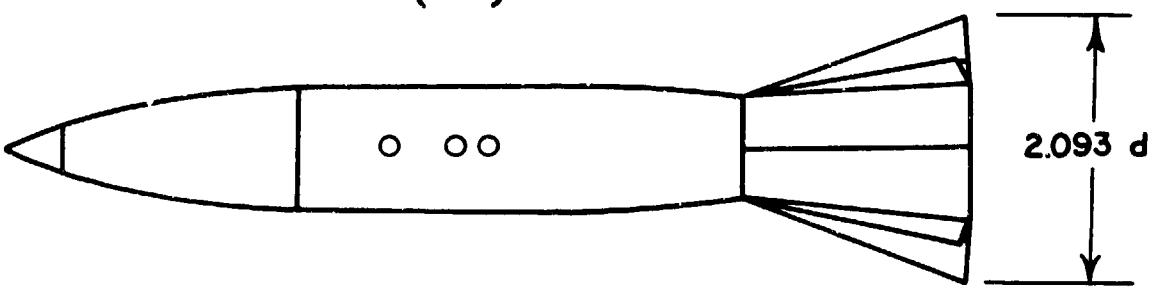

INFLATABLE STABILIZER RETARDER
(ISR)

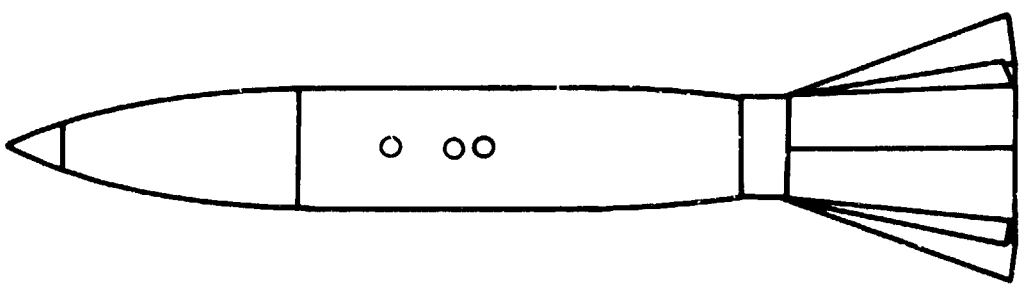

INFLATABLE STABILIZER RETARDER
EXTENDED
(ISR-E)

Figure 2. Candidate Replacements

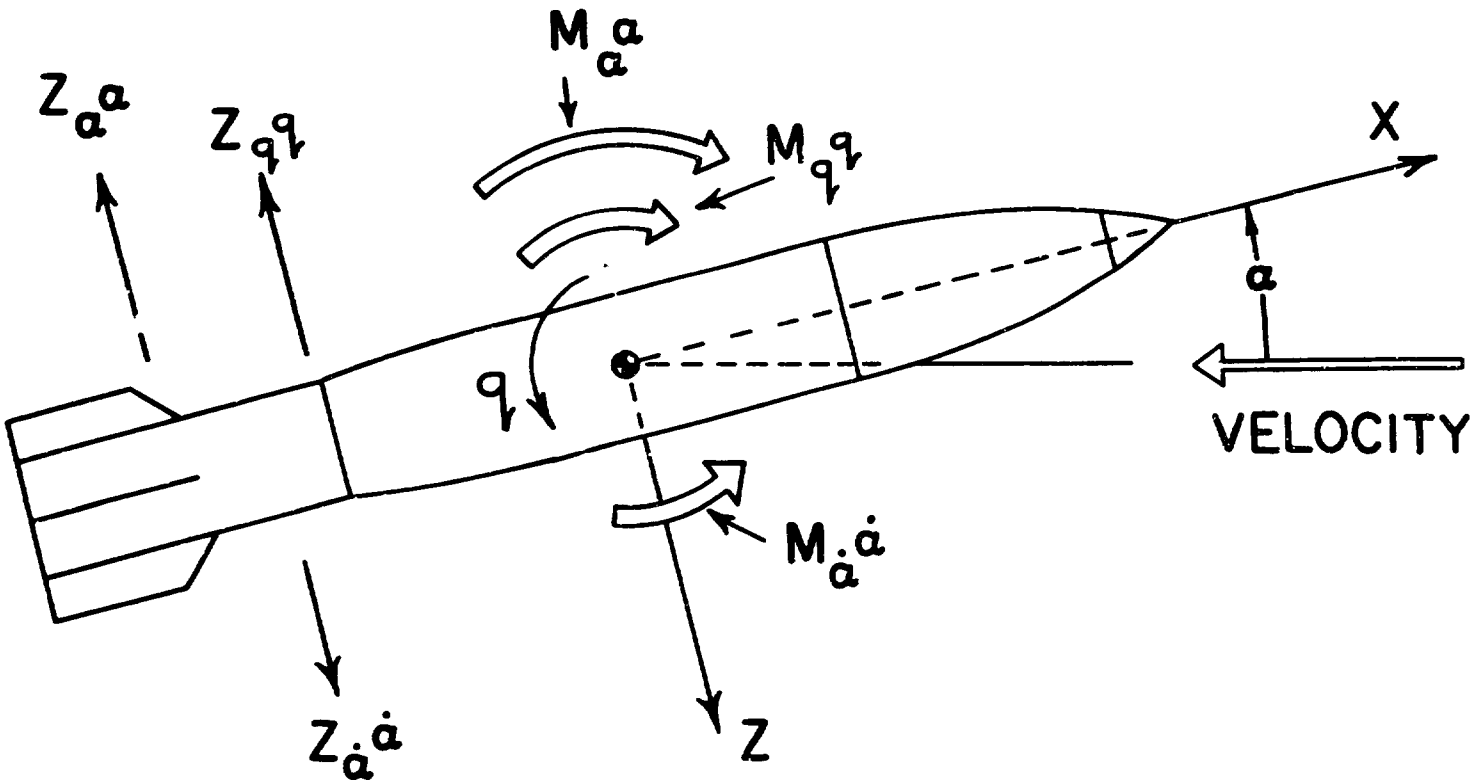

Figure 3. Single Degree of Freedom Forces and Moments

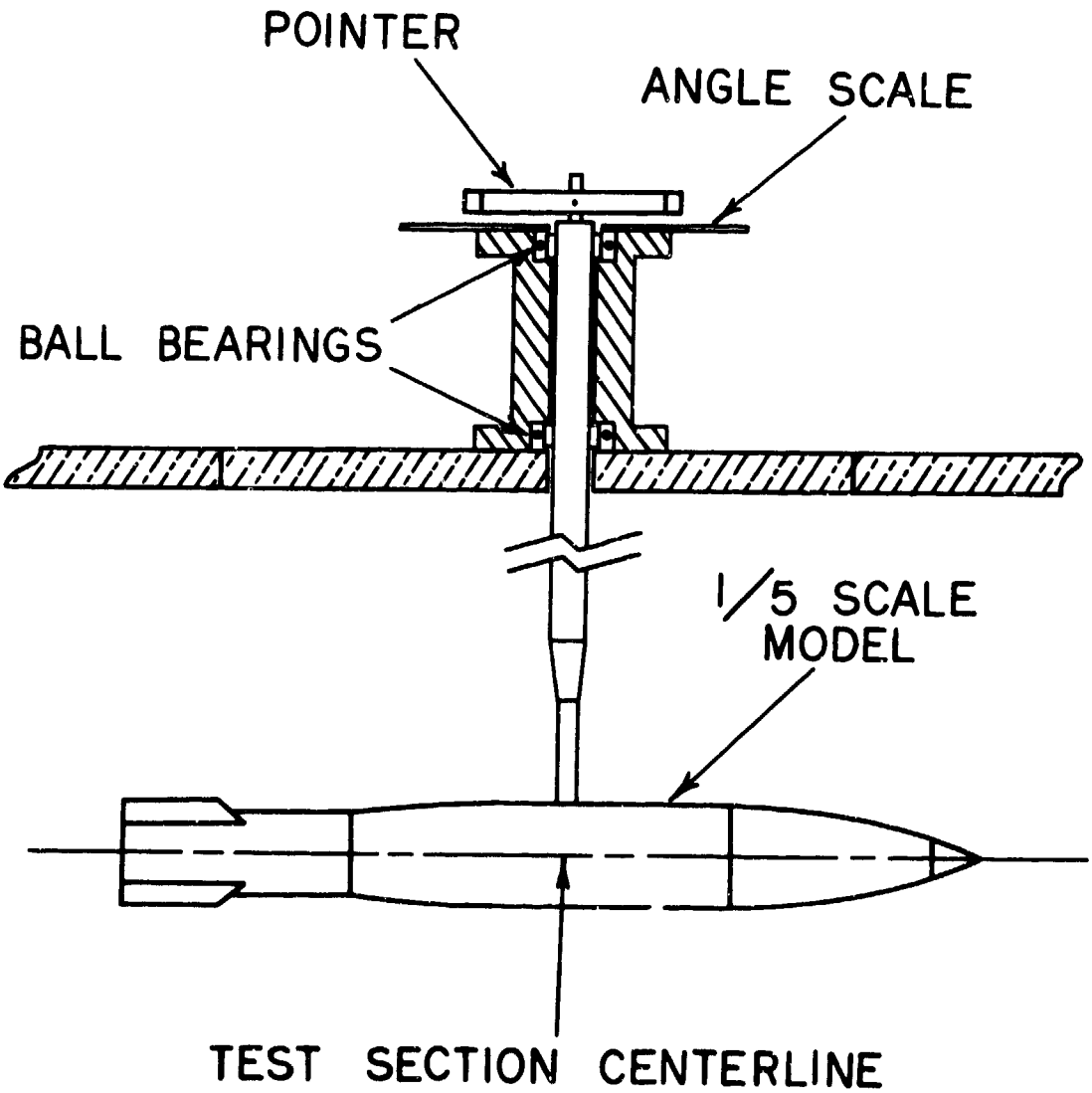

Figure 4. AFATL Model Support

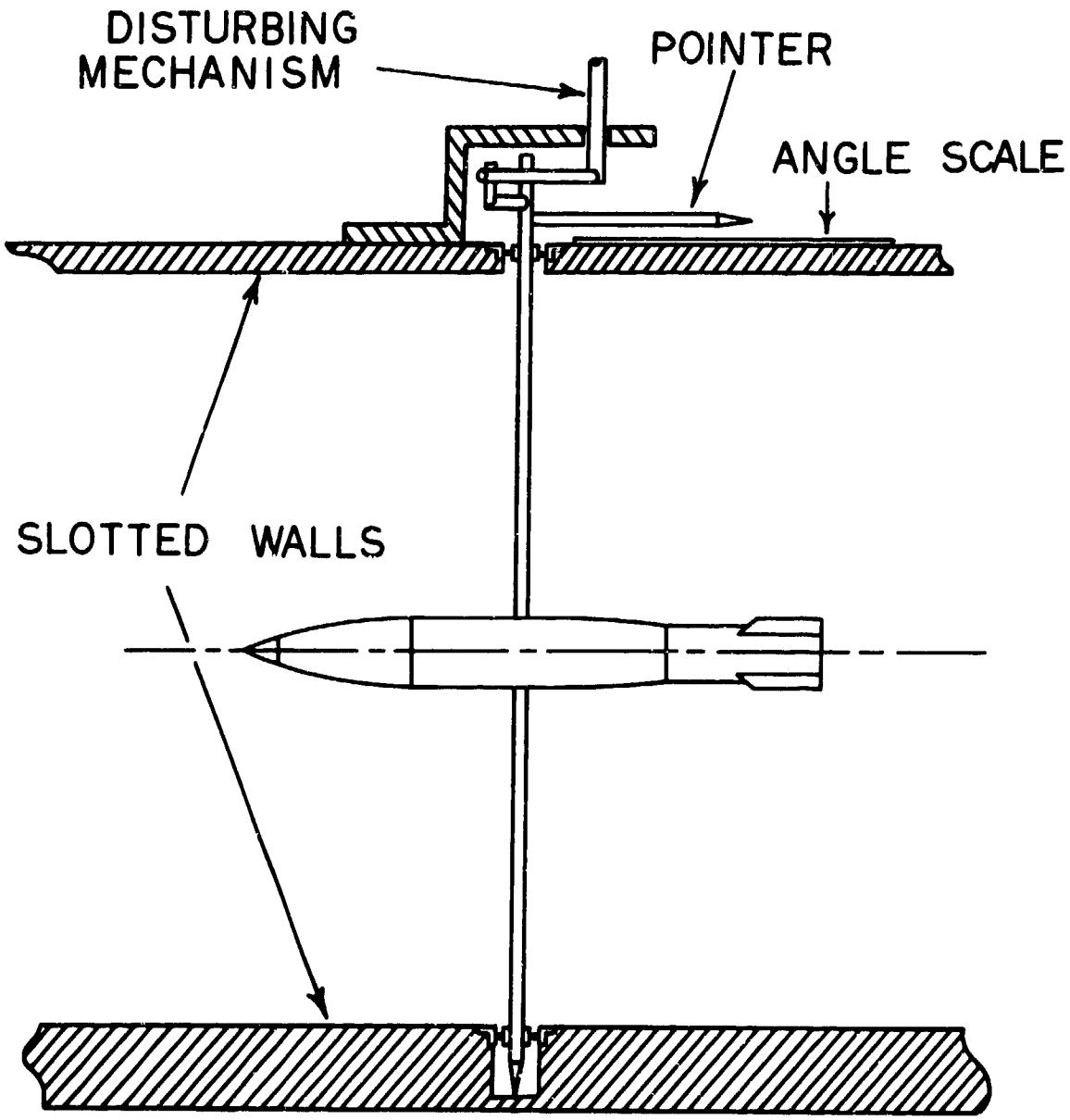

Figure 5. NSRDC Transonic Test Section

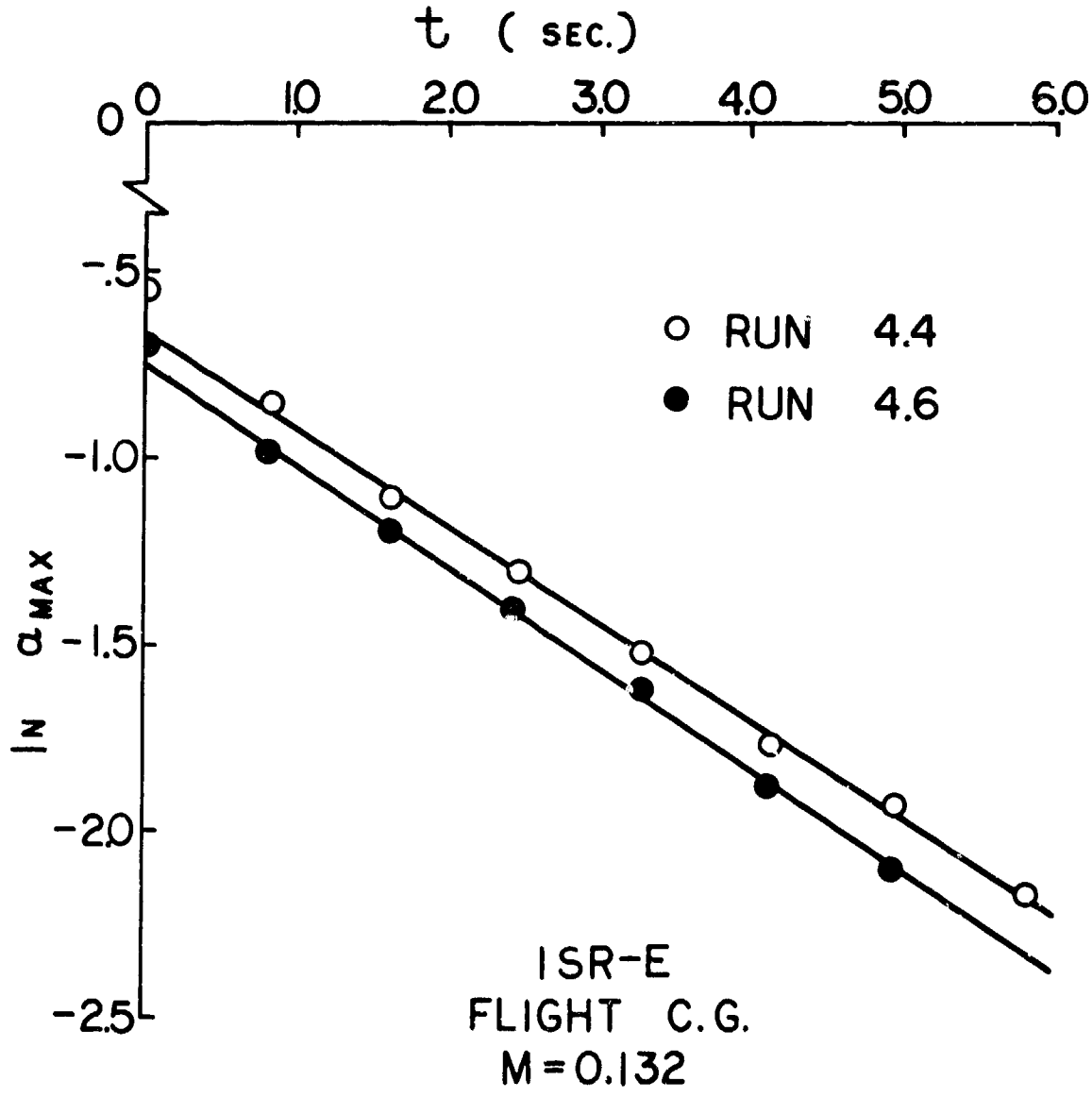

Figure 6. Sample Determination of Damping Rate

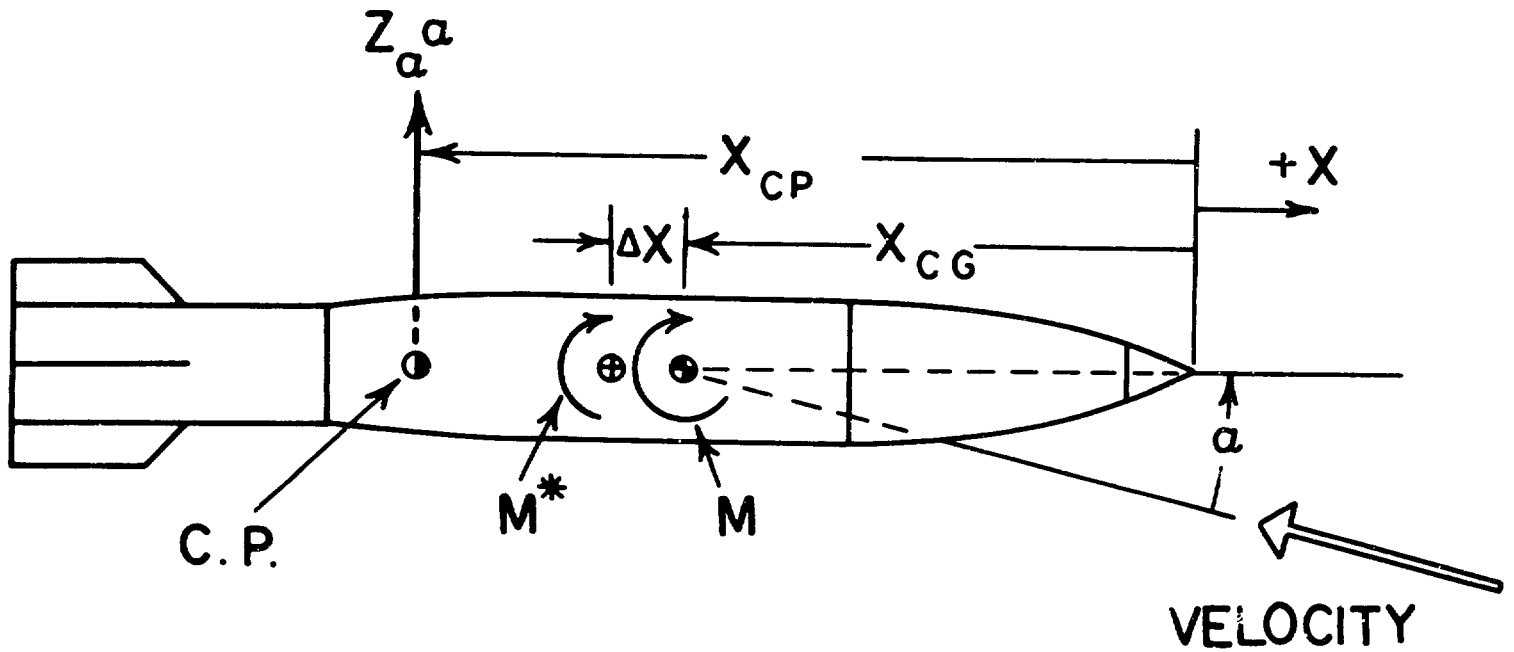

Figure 7. Nomenclature for C_{Z_α} Determination

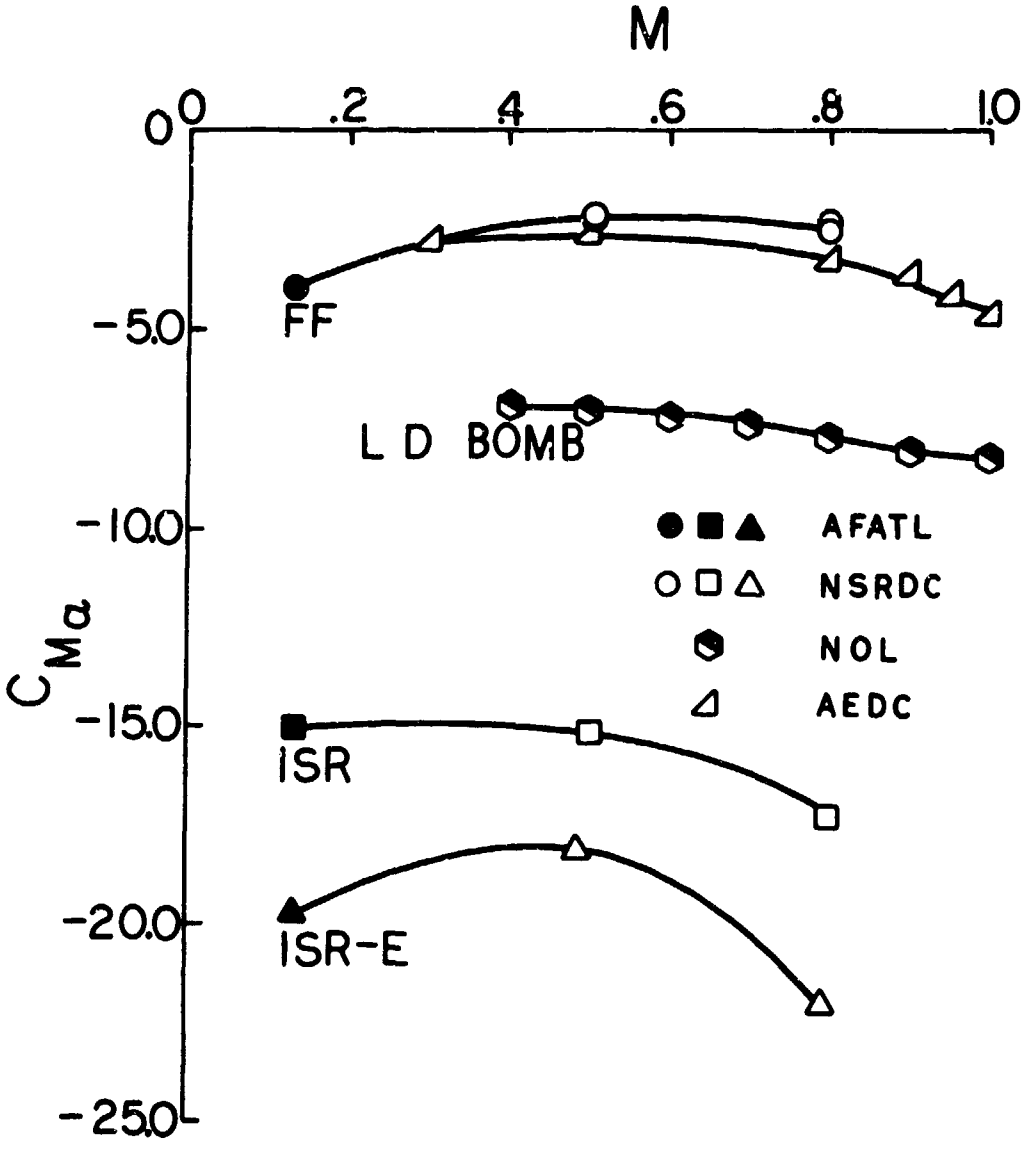

Figure 8. C_{M_α} versus M,
Flight C.G.

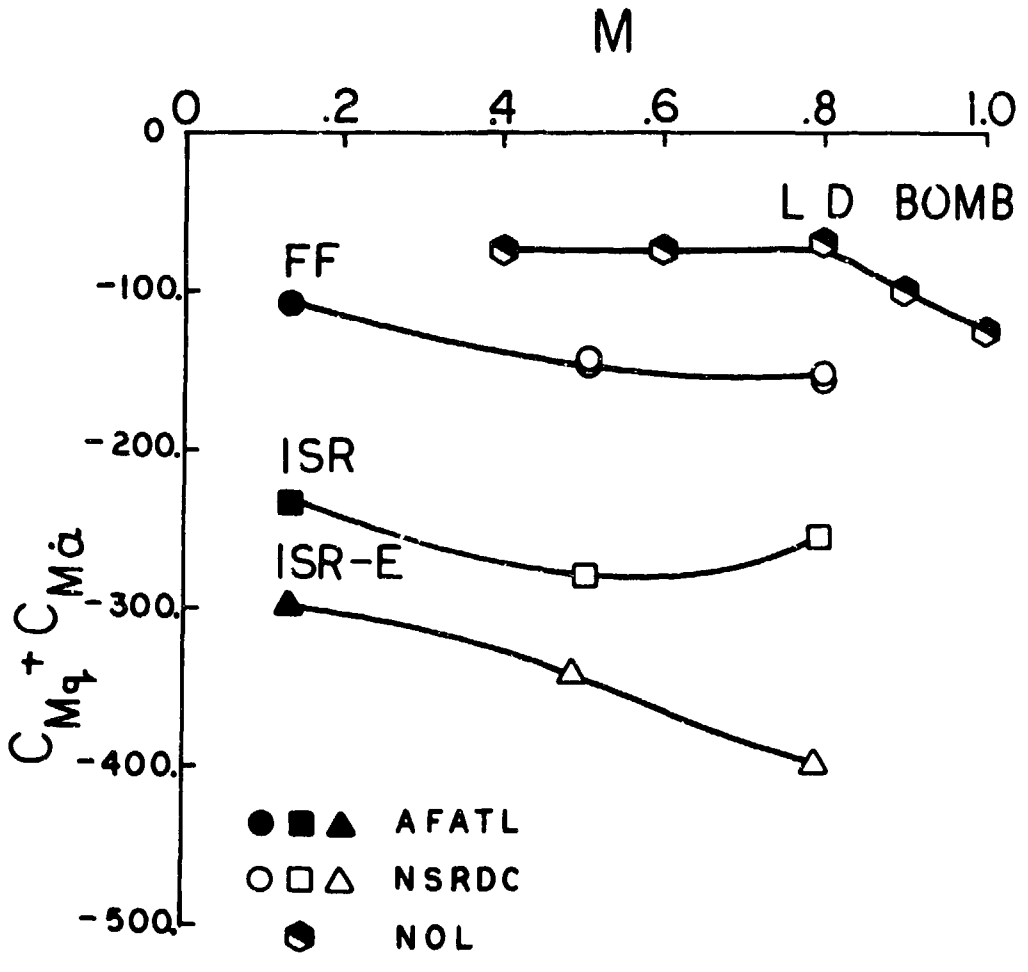

Figure 9. $C_{M_q} + C_{M_{\dot{\alpha}}}$ vs M, Flight C.G.

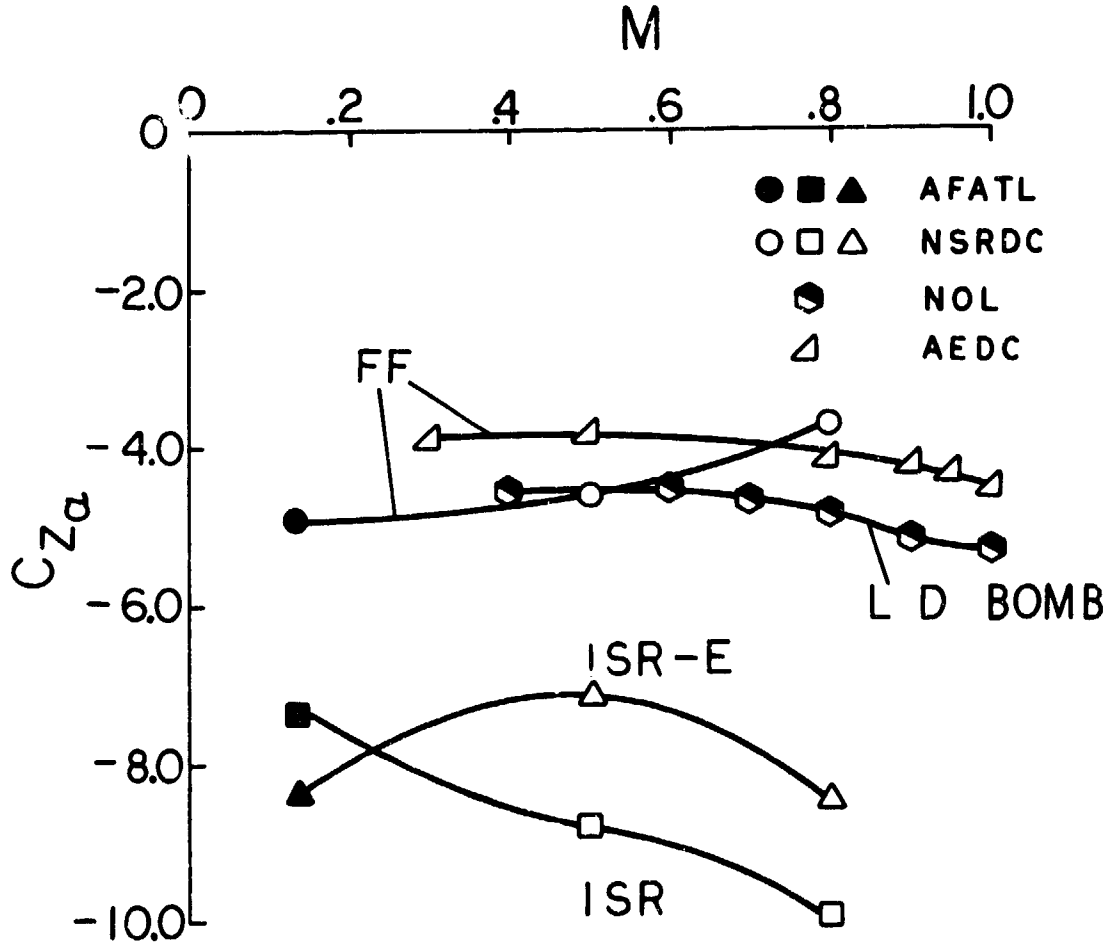

Figure 10. C_{Z_α} vs. M

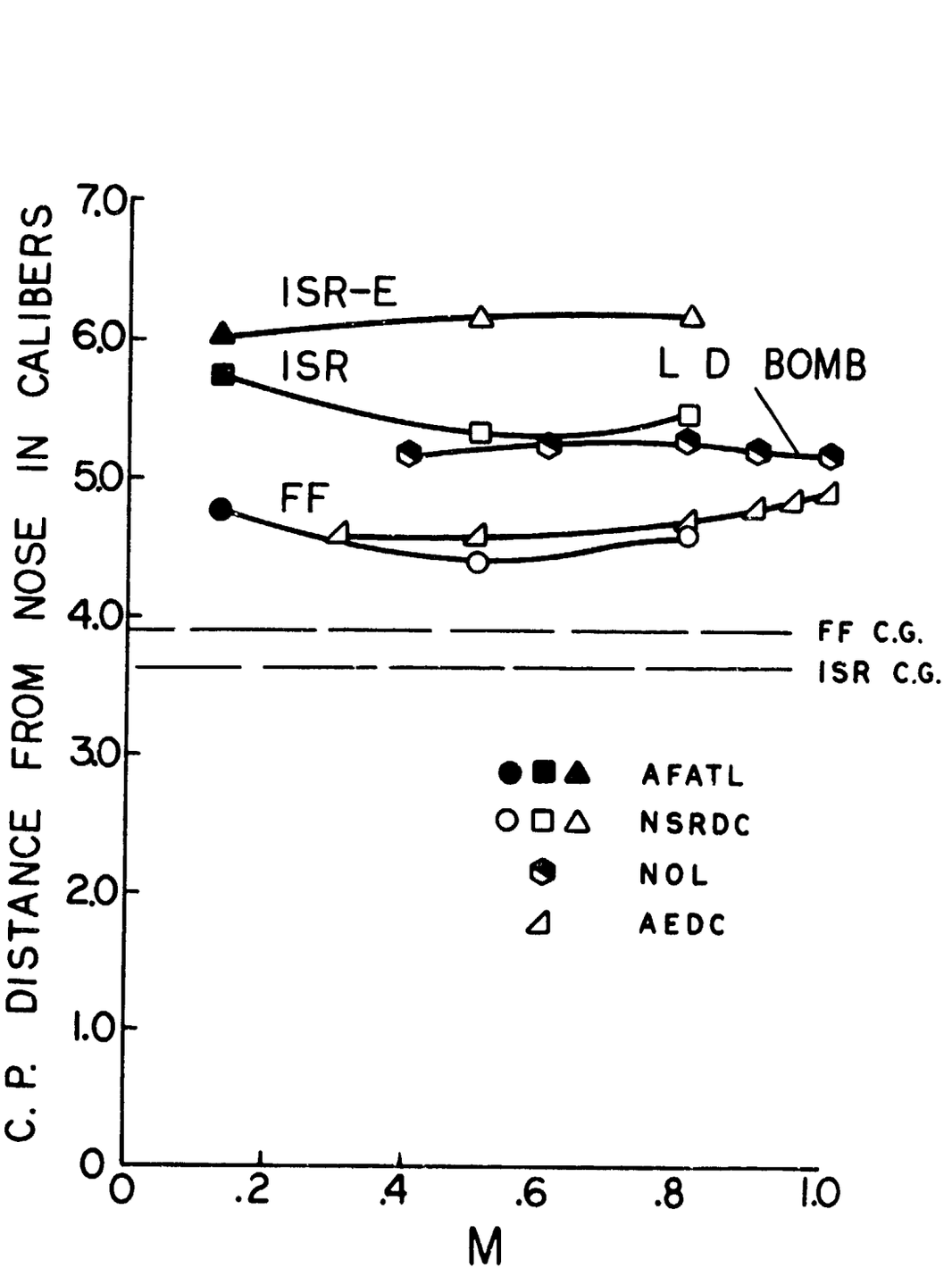

Figure 11. C.P. vs. M

REFERENCES

1. Roman, J. H., Ingram, C. W., Nicolaides, J. D., "Improvement of the Flight Performance Characteristics of the Bomb Mark 82/Snakeye Unretarded," TR-2797, Naval Weapons Laboratory, August, 1972.

2. Nicolaides, J. D., Ingram, C. W., Clare, T. A., "Investigation of the Nonlinear Flight Dynamics of Ordnance Weapons," Journal of Spacecraft, Vol. 7, No. 10, October, 1970.

3. Flatau, A., Miller, M. C., "Aeroballistic Performance Comparison of Snakeye Fins vs Ram Air Inflatable Decelerator (RAID) as Applied to MK 82 Bomb," EATM-100-12, U. S. Army Edgewood Arsenal, February 1971.

4. Evors, R. A., "Evaluation of a Ballute Retarder System for the MK 82 Bomb," ADTC-TR-73-31, U. S. Air Force Armamemt Development and Test Center, May, 1973.

5. Nicolaides, J. D., "On Missile Flight Dynamics," Ph.D. Thesis, School of Engineering and Architecture, Catholic University of America, Washington, D. C., 1963.

6. "Test Facilities Handbook (Ninth Edition)", Arnold Engineering Development Center, Arnold Air Force Station, Tenn., July, 1971.

7. Sawyer, F. M., Ingram, C. W., "In-Plane and Out-of-Plane Stability Coefficients of a Slender Biconic Reentry Vehicle at Mach 14," ARL-TR 74-0135, Aerospace Research Laboratories, 1974.

8. "Summary of MK 82 Low Drag General Purpose Bomb Aerodynamic Data," Technical Memo KEB-2, Naval Weapons Laboratory, April, 1971.

LIST OF SYMBOLS

C_M — Pitching moment coefficient

$$C_M = \frac{M}{QSd}$$

C_{M_α} — Static moment stability coefficient (radian^{-1})

$$C_{M_\alpha} = \frac{\partial C_M}{\partial \alpha} = \frac{M_\alpha \alpha}{\alpha QSd}$$

$C_{M_{\dot\alpha}}$ — Aerodynamic lag moment stability coefficient (radian^{-1})

$$C_{M_{\dot\alpha}} = \frac{\partial C_M}{\partial \frac{\dot\alpha d}{2V}} = \frac{M_{\dot\alpha}\dot\alpha}{\frac{\dot\alpha d}{2V} QSd}$$

C_{M_q} — Damping moment stability coefficient (radian^{-1})

$$C_{M_q} = \frac{\partial C_M}{\partial \frac{qd}{2V}} = \frac{M_q q}{\frac{qd}{2V} QSd}$$

C_Z — Normal Force Coefficient

$$C_Z = \frac{Z}{QS}$$

C_{Z_α} — Normal Force Coefficient slope (radian^{-1})

$$C_{Z_\alpha} = \frac{\partial C_Z}{\partial \alpha} = \frac{Z_\alpha \alpha}{\alpha QS}$$

d — Diameter of bomb forebody (feet)

I — Total moment of inertia (slug foot^2)

$$I = I_y + I_{X\ \text{mount}}$$

I_y — Transverse moment of inertia of model (slug foot^2)

M — Pitch moment (foot pounds)

$$M = C_M QSd$$

M_α — Restoring moment stability derivative (foot pound/radian)

$$M_\alpha = C_{M_\alpha} QSd$$

$M_{\dot\alpha}$ — Aerodynamic lag moment stability derivative (foot pound second/radian)

$$M_{\dot\alpha} = C_{M_{\dot\alpha}} \frac{d}{2V} QSd$$

M_q	Damping moment stability derivative (foot pound second/radian) $M_q = C_{M_q} \frac{d}{2V} QSd$
q	Pitching angular velocity (radian/second)
Q	Dynamic Pressure (pound/foot^2) $Q = \frac{1}{2} \rho V^2$
S	Frontal area (feet^2) $S = \pi d^2/4$
t	Time (seconds)
T	Period of oscillation (seconds)
V	Total velocity (feet/second)
X	Distance measured along centerline of body (feet)
Z_α	Static force per radian of angle of attack (pound/radian)
$Z_{\dot{\alpha}}$	Aerodynamic lag normal force per radian/second of angular rate (pound second/radian) $Z_{\dot{\alpha}} = C_{Z_{\dot{\alpha}}} \frac{d}{2V} QS$
Z_q	Damping normal force per radian/second of angular rate (pound second/radian) $Z_q = C_{Z_q} \frac{d}{2V} QS$

Greek

α	Angle of attack (radians)
α_m	Maximum angle of attack (radians)
α_0	Initial angle of attack (radians)

LIST OF SYMBOLS (continued)

δ	Phase angle (radians)
λ	Damping rate of single degree of freedom motion (second^{-1})
ρ	Air density (slug/foot^3)
ω	Angular rate of single degree of freedom motion (radian/second)

Derivatives

$(\dot{})$	First time derivative (second^{-1})
	$(\dot{}) = \frac{d}{dt}\ (\ )$
$(\ddot{})$	Second time derivative (second^{-2})
	$(\ddot{}) = \frac{d^2}{dt^2}\ (\ )$

*U.S.Government Printing Office 1975 — 657-023/714